

**Supplementary information for**

5

**A novel pulse isotopic exchange technique for rapid determination of the oxygen  
surface exchange rate of oxide ion conductors**

Henny J.M. Bouwmeester,<sup>\*</sup> Chunlin Song, Jianjun Zhu, Jianxin Yi, Martin van Sint Annaland and  
10 Bernard A. Boukamp

Faculty of Science and Technology, MESA<sup>+</sup> Institute for Nanotechnology & IMPACT Institute of  
Mechanics, Processes and Control Twente, University of Twente, PO Box 217, 7500 AE Enschede,  
The Netherlands

15 <sup>\*</sup> E-mail: [h.j.m.bouwmeester@tnw.utwente.nl](mailto:h.j.m.bouwmeester@tnw.utwente.nl)

## Experimental details

YSZ powder (TOSOH, Japan, purity 99.9%) was calcined in air at 900 °C for 10 h. BSCF powder, prepared by spray pyrolysis, was calcined in air at 800 °C for 24 h, and subsequently ball-milled in ethanol. After calcination, the powder was uniaxially pressed at 25MPa into a disc, followed by isostatically pressing at 400 MPa. After sintering in air at 1100 °C for 10 h, the obtained dense disc was crushed into a powder. The powder was then sieved through a 120 mesh metal screen. Prior to use, the powder was again calcined in air at 950 °C for 10 h and sieved through the 120 mesh metal screen to remove formed agglomerates.  $\text{La}_2\text{NiO}_{4+\delta}$  was prepared by thermal decomposition of precursor complexes derived from nitrate solution using ethylene-diamine-tetra-acetic (EDTA) as a complexing agent. The powder thus obtained was calcined in air at 1000°C for 10 h. After calcination, the powder was ball-milled in acetone for 5 h. The remainder of the procedure is similar to that described for BSCF, except for changes in the temperatures of sintering and subsequent calcination of the powder obtained from crushing the sintered disc to 1370 and 1100 °C, respectively. The relative densities were above 94% for all sintered specimens. X-ray powder diffraction confirmed that in all cases the desired structures were formed. Within the detection limit of the diffractometer, no evidence for second phase formation was found. For YSZ,  $\text{La}_2\text{NiO}_{4+\delta}$  and BSCF powders, the particle sizes were in the range 2.0-5.0  $\mu\text{m}$ , with BET surfaces 10.12, 0.156 and 0.210  $\text{m}^2\text{g}^{-1}$ , respectively.

Pulse oxygen isotope exchange experiments were conducted in the temperature range 350-900 °C, using a continuous-flow packed-bed micro-reactor. Quartz wool plugs were used to support and secure 20-100 mg of the oxide powder in the centre of the quartz tubular reactor with inner diameter of 2 mm. The length of the packed bed varied between 6-20 mm, and typically was 10 mm. A  $^{16}\text{O}_2/\text{He}$  gas mixture with a total flow rate of 50 (STP)  $\text{ml}\cdot\text{min}^{-1}$  was used as carrier gas. Prior to pulsing isotopically labeled oxygen through the reactor, the sample was flushed with the carrier gas at 850 °C for 2 h to remove possible adsorbates (such as  $\text{CO}_2$ ). Next, the system was cooled to room temperature. The response to a pulse of  $^{18}\text{O}_2$ -enriched  $\text{N}_2$  gas (500  $\mu\text{l}$ ) through the reactor was analyzed at the reactor exit by on-line quadrupole mass spectrometry (OmniStar™ GSD 301, Pfeiffer-Vacuum). Measurements were made from room temperature onwards. Oxygen isotope gas was purchased from Sigma-Aldrich (> 99 atom%  $^{18}\text{O}_2$ ). While helium was used as the diluent for  $^{16}\text{O}_2$  in the carrier gas, nitrogen was used as the diluent for the isotope gas acting as an internal reference for mass spectrometry. Both carrier and pulse gases were diluted to the same oxygen partial pressure ( $p\text{O}_2 = 0.21 \text{ atm}$ ). A 6-port valve was used to inject the  $^{18}\text{O}_2/\text{N}_2$  pulse into the  $^{16}\text{O}_2/\text{He}$  carrier gas flow stream. The number of  $^{18}\text{O}$  atoms in the pulse typically remained below 1% of the number of oxygen atoms

present in the oxide sample. Mean residence times varied from 5 to 40 ms. The sample was equilibrated 15 min at each temperature before conducting the pulse response measurements. Blank experiments revealed no exchange activity of the quartz micro-reactor.

5 **Supplementary Fig. S1**

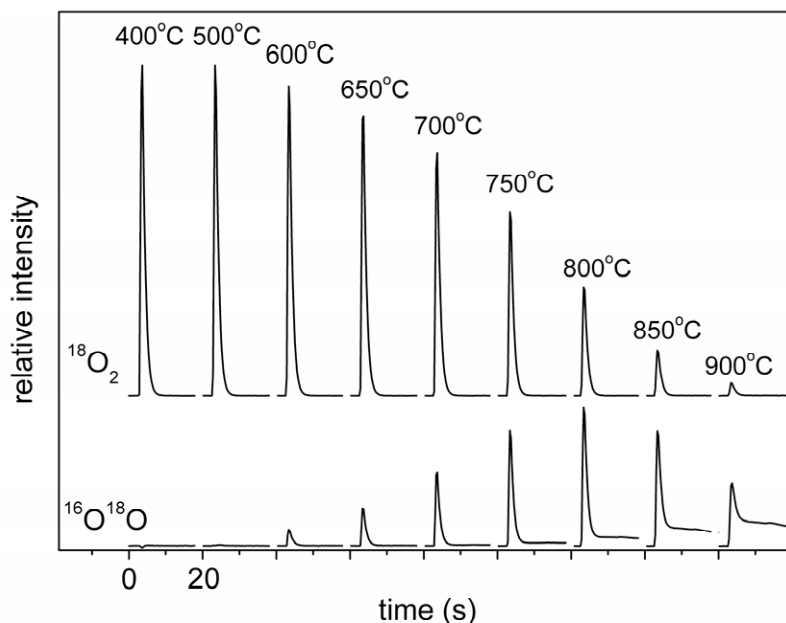


**Fig. S1.** Raw mass spectroscopic data from pulse-response isotopic exchange measurements on YSZ powder. Peak data at different temperatures are shifted with respect to each other for reasons of clarity. Note that at given experimental conditions peak tailing is observed for the  $^{16}\text{O}^{18}\text{O}$  peak acquisition at the highest temperatures. Tailing is due to the high oxygen exchange rate at elevated temperatures, and is only manifest for the  $^{16}\text{O}^{18}\text{O}$  peak. The latter is caused by the recombination of exchanged  $^{18}\text{O}$  with excess  $^{16}\text{O}$  from the oxide, followed by the release of the  $^{16}\text{O}^{18}\text{O}$  molecule to the gas phase.

## Plug flow reactor

The assumption of ideal plug flow behaviour implies that criteria need to be fulfilled for neglecting the effect of axial dispersion and the packing-disrupted and, consequently, higher gas velocity near the reactor wall:  $L/d_p > 50$  and  $d_t/d_p > 10$ , respectively, where  $L$  is the bed length,  $d_p$  the particle diameter and  $d_t$  the reactor diameter. Care was taken to ensure the validity of these and other design criteria by following the recommendations as, for example, provided in Ref. 1. Mainly due to the small grain sizes of the powders,  $L/d_p$  and  $d_t/d_p$  associated with our experiments are well in excess of the above set minimum values for these ratios, ranging from  $L/d_p = 1290$  and  $d_t/d_p = 410$  for YSZ ( $L = 6.9$  mm,  $d_p = 4.9$   $\mu\text{m}$ ,  $d_t = 2.0$  mm) to  $L/d_p = 7500$  and  $d_t/d_p = 1000$  for  $\text{La}_2\text{NiO}_{4+\delta}$  ( $L = 15.0$  mm,  $d_p = 2.0$   $\mu\text{m}$ ,  $d_t = 2.0$  mm). Because of the low particle Reynolds numbers  $Re_p$  ( $\sim 0.065$ ), the axial dispersion in our packed bed reactor is dominated by molecular diffusion.<sup>2</sup> The Péclet number  $Pe = \langle v \rangle d_t / D_1$ , where  $\langle v \rangle$  = the average velocity of the gas phase and  $D_1$  the longitudinal or axial dispersion coefficient, is calculated at a value of  $\sim 160$  at 500 °C, confirming that axial dispersion should be sufficiently limited to justify the use of the ideal plug flow model.<sup>2</sup> In calculation,  $D_1$  has been approximated by the estimate from Fuller's equation used for calculation of the binary diffusion coefficient of  $\text{O}_2\text{-N}_2$ .<sup>3</sup> Additionally, diagnostic tests were carried out to check the validity of the plug flow criteria by varying the residence time through variation of the volumetric flow rate or length of the packed bed in ranges 25-100 (STP)  $\text{ml}\cdot\text{cm}^{-1}$  and 6-20 mm, respectively, during measurement of the surface exchange rates. The average residence time was calculated from  $\tau_r = (V_b \varepsilon / F)$ , where  $V_b$  is the total volume of the packed bed,  $\varepsilon$  the corresponding bed porosity, and  $F$  the volumetric flow rate, which equation can be converted to conditions corresponding to the audit flow rate  $F_0$ :  $\tau_r = (V_b \varepsilon / F_0) \cdot (T_0 / T)$ . No significant differences in the calculated exchange rates extracted from these experiments were found. Evidence of external mass transfer limitations was found in some cases for relatively large porous particles, due to the surface-associated increase of the exchange rate. Intrapore and/or extraparticle mass transport limitations could be avoided by the use of crushed sintered, i.e. non-porous, samples for the experiments.

Finally, it should be noted that many studies of high-temperature oxygen transport in fast oxide-ion conducting ceramics have revealed that the characteristic length scale,  $L_c$ , below which oxygen exchange is governed by the surface reaction rather than by bulk oxygen diffusion, varies between 10  $\mu\text{m}$  up to the cm range.<sup>4</sup> This range is distinctly higher than that of the particle sizes used in our experiments. It may be further recalled that the total number of  $^{18}\text{O}$  atoms in the pulse is below  $\sim 1\%$  of the number of oxygen atoms present in the oxide sample. In view of these facts, severe accumulation

of  $^{18}\text{O}$  in the oxide near-surface region is not expected which, in case of occurrence, would lead to a violation of the boundary condition used to derive Equation 2.

1 J. Pérez-Ramírez, R.J. Berger, G. Mul, F. Kapteijn and J.A. Moulijn, *Catal. Today* 2000, **60**, 93.

2 K.R. Westerterp, W.P.M. van Swaaij and A.A.C.M. Beenhakkers, in *Chemical Reactor Design and Operation*, John Wiley & Sons Ltd., Chichester, 2<sup>nd</sup> edn., 1984, ch. 4, pp. 160-226.

3. For example, see R.C. Reid, J.M. Prausnitz, B.E. Poling, in *The properties of gases and liquids*, McGraw-Hill, Inc. New York, 4th edn., 1987, pp. 587-588

4 J.A. Kilner and R.A. De Souza, *Solid State Ionics* 1999, **126**, 153.

10

### Model Equations

Expressions for the molar gas phase fractions of  $^{18}\text{O}_2$ ,  $^{16}\text{O}^{18}\text{O}$  and  $^{16}\text{O}_2$  in the pulse volume at the exit of the reactor were derived from our previous work.<sup>5</sup> With the notion that during passage of the  $^{18}\text{O}$ -enriched pulse through the packed bed the corresponding fraction in the oxide remains virtually zero,  
 15 one finds for the gas phase fraction of  $^{18}\text{O}_2$ ,

$$f_{g,e}^{36} = \left( \frac{(1-p)}{(1-2p)^{1/2}} \cdot f_{g,i}^{18} \right)^2 \cdot \exp\left(-\frac{2 \cdot \tau_r}{\tau_u}\right) + \left( f_{g,i}^{36} - \left( \frac{(1-p)}{(1-2p)^{1/2}} \cdot f_{g,i}^{18} \right)^2 \right) \cdot \exp\left(-\frac{\tau_r}{\tau_u p}\right)$$

where  $p = \mathfrak{R}_i / (\mathfrak{R}_a + \mathfrak{R}_i)$  and  $\tau_u = n / \mathfrak{R}_0 S$ . The parameter  $p$  reflects the probability of incorporation into  
 20 the oxide lattice during its residence time at the oxide surface. The meaning of other parameters is explained in the main text. The molar fractions with mass numbers 34 ( $^{16}\text{O}^{18}\text{O}$ ) and 32 ( $^{16}\text{O}_2$ ) are calculated using the relationships:  $f_g^{18} = f_g^{36} + 0.5 f_g^{34}$  and  $f_g^{32} + f_g^{34} + f_g^{36} = 1$ .

5 M.W. Den Otter, B.A. Boukamp and H.J.M. Bouwmeester, *Solid State Ionics* 2001, **139**, 89

25

30

## Supplementary Fig. S2

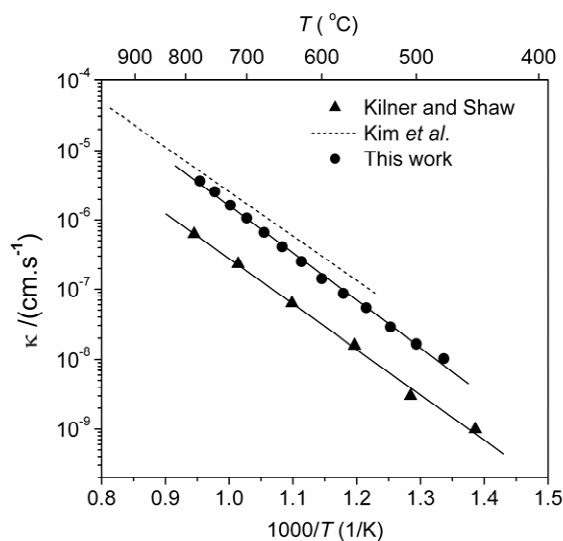


**Fig. S2.** Comparison of the oxygen surface exchange rate,  $k^*$ , for  $\text{La}_2\text{NiO}_{4+\delta}$  as obtained by pulse isotopic exchange measurements with those from previous studies on dense ceramic samples using electrical conductivity relaxation<sup>6</sup> and isotopic exchange depth profiling (IEDP).<sup>7</sup> To enable comparison, the surface exchange rate from this study was re-calculated using  $k^* = \mathfrak{R}_0/c_{\text{O}}$ , where  $c_{\text{O}}$  is the concentration of oxygen ions in the oxide.

<sup>6</sup> G. Kim, S. Wang, A.J. Jacobson, L. Reimus, P. Brodersen and C.A. Mims, *J. Mater. Chem.* 2007, **17**, 2500.

<sup>7</sup> J.A. Kilner and C.K.M. Shaw, *Solid State Ionics* 2002, **154-155**, 523,